Impact of papillary muscle infarction on atrial and ventricular myocardial deformation in non-anterior STEMI patients

Riccardo Cau[1], Alessandro Pinna[1], Roberta Montisci[2], Luigia d'Errico[3], Jasjit S. Suri[4] , Marco Francone[5,6], Giuseppe Muscogiuri[7], Luca Saba[1]

[1]Department of Radiology, Azienda Ospedaliero Universitaria (A.O.U.), di Cagliari – Polo di Monserrato s.s. 554 Monserrato (Cagliari) 09045, ITALY

[2] Department of Cardiology, Azienda Ospedaliero Universitaria (A.O.U.), di Cagliari – Polo di Monserrato s.s. 554 Monserrato (Cagliari) 09045, ITALY

[3] Department of Medical Imaging, University Health Network, University of Toronto, Toronto, Ontario, Canada

[4] Stroke Monitoring and Diagnostic Division, AtheroPoint™, Roseville, CA 95661, USA

[5] IRCCS Humanitas Research Hospital, Via Manzoni 56, Rozzano, Italy

[6]Department of Biomedical Sciences, Humanitas University, Pieve Emanuele, Italy

[7] Department of Radiology, ASST Papa Giovanni XXIII Hospital, Bergamo, Italy

Corresponding author: Luca Saba MD, telephone +393280861848, fax +39070485980, email: lucasaba@tiscali.it ; Department of Radiology, Azienda Ospedaliero Universitaria (A.O.U.), di Cagliari – Polo di Monserrato s.s. 554 Monserrato (Cagliari) 09045, ITALY

Abstract

Objective: The purpose of this study was to explore the impact of papillary muscle (PPM) infarction on left atrial and ventricular strain parameters in patients with non-anterior ST-segment elevation myocardial infarction (NA-STEMI) using cardiovascular magnetic resonance (CMR).

Method: This retrospective study performed CMR scans on 88 consecutive patients with NA-STEMI (68 males, 65 ± 10.05 years). Among them, 30 demonstrated PPM infarction (25 males, 67.12 ± 9.49 years), defined as late gadolinium enhancement (LGE) in a papillary muscle head in two contiguous LGE CMR slices, and confirmed on the long-axis LGE CMR slices. Atrial and ventricular strain were analyzed by CMR feature tracking with dedicated post-processing software

Results: Patients with PPM infarction were older ($p = 0.001$), with lower left ventricular ejection fraction ($p = 0.040$), higher indexed left ventricular end-diastolic volume ($p = 0.020$), and end-systolic volume ($p = 0.044$) compared to patients without LGE in the papillary muscle. Additionally, patients with PPM infarction showed impaired reservoir strain, booster strain, global longitudinal strain (GLS), and higher LGE extent compared to NA-STEMI patients without PPM involvement ($p = 0.001$, $p = 0.004$, $p = 0.001$, and $p = 0.003$, respectively). In multivariable analysis, GLS, global radial strain, reservoir strain, and booster strain parameters were the only independent determinants of PPM infarction ($p = 0.001$, $p = 0.041$, $p = 0.002$, and $p = 0.027$, respectively)

Conclusion: The presence of PPM infarction assessed by CMR is independently linked to atrial and ventricular strain impairment in patients with NA-STEMI

Abbreviations

CMR cardiovascular magnetic resonance

LGE late gadolinium enhancement

LV left ventricle

PPM papillary muscle

NA-STEMI non-anterior ST-segment elevation myocardial infarction

Keywords: STEMI; myocardial strain; CMR; papillary muscle infarction

Highlights

- Papillary muscles play an integral role in cardiac function.
- Papillary muscle infarction is a relatively common complication of myocardial infarction.
- Papillary muscle dysfunction leads to impaired atrial and ventricular strain

Introduction

The left ventricular papillary muscles (PPMs) are muscular structures that arise from the ventricular wall, influencing ventricular geometry and function. They play an integral role in cardiac mechanics: during diastole, they limit left ventricular distension, and during systole, they enhance longitudinal shortening. This action increases left ventricular wall stress, leading to greater contractile force and stroke volume[1,2].During acute myocardial infarction, necrosis can extend into one or both papillary muscles, altering myocardial contraction[3].

Cardiac magnetic resonance imaging (CMR) is a key technique for evaluating the PPMs, offering detailed information on their morphology, function, and tissue characteristics[4]. Late gadolinium enhancement (LGE) imaging has become the gold standard for detecting even small areas of

myocardial necrosis in vivo, including necrosis in the papillary muscles[5–9], thank also to dedicated gray-blood LGE sequences[10].

PPM infarction has been shown to have a negative prognostic value and is associated with an increased cardiovascular mortality rate[3]. Therefore, identifying the determinants of PPM infarction and delineating the possible underlying mechanisms related to adverse outcomes in non-anterior ST-segment elevation myocardial infarction (NA-STEMI) patients is crucial. This may help to better stratify patients after myocardial infarction.

Myocardial strain measures the rate of myocardial deformation between the relaxed and contracted states during a cardiac cycle in both the atrial and ventricular chambers, and it can non-invasively detect abnormal myocardial contraction resulting from PPM infarction[6,11–14].

This study aimed to investigate the impact of PPM infarction on left atrial and ventricular parameters in patients with NA-STEMI using CMR.

Material and Method

Study population

In this retrospective, cross-sectional, observational, single-center study, all consecutive patients with NA-STEMI who underwent CMR between March 3rd 2019, and December 31st 2023 were included.

STEMI was defined according to the ESC/ACCF/AHA/WHF consensus document criteria, which include typical chest pain lasting more than 30 minutes, persistent ST-segment elevation of at least 1.0 mm in two or more contiguous ECG leads, and elevated cardiac enzyme levels[15].

Non-anterior STEMI was characterized by ST-segment elevation in the lateral (V5, V6, I, aVL), inferior (II, III, aVF), or inferolateral (I, II, III, aVF, V5, V6) ECG leads, or by a posterior myocardial infarction indicated by ST depression of 1 mm or more in at least two contiguous anterior leads[16].

Exclusion criteria included: subjects < 18 years; previous myocardial infarction; pre-existing cardiomyopathy; known valvular diseases: and suspected or known prior irreversible myocardial damage.

Cardiovascular risk factors were collected from medical records. Hypertension was defined as a systolic blood pressure of ≥140 mmHg or a diastolic blood pressure of ≥ 90 mmHg at rest on more than two occasions, or the use of antihypertensive drugs[17]. Smoking status was defined as current smokers or never smokers. Cholesterol laboratory analyses were conducted following the standard in-house protocol. Diabetes status was assessed using the World Health Organization criteria[18] or an established diagnosis of type 2 diabetes. Obesity was defined as a BMI > 30, as defined by the World Health Organization criteria[19].

The Institutional Review Board approval for this retrospective, cross-sectional study was obtained, and patient's consent was waived because of the retrospective nature.

A flowchart demonstrating the application of inclusion and exclusion criteria is provided in **Figure 1.**

CMR acquisition

CMR scans were performed at 10.2±3.5 days after coronary revascularization by using a Philips Achieva dStream 1.5 T scanner system (*Philips Healthcare, Best, The Netherlands*). Anterior coil arrays were used. All cine-images were acquired using a balanced steady-state free precession and retrospective gating during an expiratory breath- hold manoeuvres (TE: 1.7mssec; TR: 3.4msec /flip-angle: 45°, section thickness = 8 mm) in both long-axis (two-, three- and four-chamber view) as well as short-axis plane with whole ventricular coverage from left ventricle (LV) base to apex.

LGE imaging was performed in both long- and short- axis slices 10–12 min after contrast media injection (Gadovist, Bayer Healthcare) with a dose of 0.15 ml per kg body weight using phase-

sensitive inversion recovery sequences (PSIR) (TE: 2.0 ms; TR: 3.4 ms; flip angle: 20°, section thickness = 8 mm) with an inversion time deter- mined using the Look-Locker technique. A free-breathing, ECG-triggered, phase-contrast velocity-encoded CMR sequence of the aortic outflow was acquired using cine images in the three-chamber orientation and LVOT to plan the acquisition of the flow images (TE 3.8 ms; TR 13.4 ms; FOV 240–320 mm; matrix = 77 × 128).

CMR image post-processing

We used the commercially available software system Circle CVI42 (*CVI42, Circle Cardiovascular Imaging Inc., Calgary, Canada*) for CMR-FT data analysis. LV volumes and function were determined on short-axis cine images by manually tracing contours. LV end-diastolic volume and end-systolic volume were obtained from the cine images. The LV ejection fraction (EF) was calculated using the formula: (LV end-diastolic volume – LV end-systolic volume) / LV end-diastolic volume * 100%.

Offline CMR feature tracking analyses were performed to evaluate peak global longitudinal strain, global radial strain, and global circumferential strain using a 16-segment, software-generated 2D model. Longitudinal strain data were derived from two-, three-, and four-chamber long-axis views, while radial and circumferential strain data were obtained from apical, mid-ventricular, and basal short-axis views in all patients. The epi- and endocardial borders were traced in end-diastole on all images, after which an automatic computation was initiated to outline the borders throughout the cardiac cycle. The quality of tracking and contouring was visually validated and manually corrected as needed.

CMR feature tracking analyses of atrial deformation were also conducted offline. The LA endocardial borders were manually traced on long-axis views of the cine images when the atrium was at its minimum volume. Specifically, the four-, three-, and two-chamber views were used to derive LA longitudinal strain, excluding the LA appendage and pulmonary veins. After manual

segmentation, the software automatically tracked the myocardial borders throughout the entire cardiac cycle. The quality of tracking and contouring was visually validated and manually corrected by a radiologist with three years of experience in cardiac imaging. The strain curve included three peaks: reservoir, conduit, and booster strain.

PPM infarction was assessed visually and semiquantitatively by a blinded expert observer with more than 7 years of experience in cardiovascular imaging. The presence of PPM infarction was defined as LGE in a papillary muscle head in 2 contiguous LGE CMR slices, and its presence needed to be confirmed on the long-axis LGE CMR slices. Cine images of the same locations served as side-by-side references to help locate the papillary muscle within the blood pool during the interpretation of contrast-enhanced images[20]. **Figure 2**

The LGE extension was evaluated semiquantitatively, as the number of segments with ischemic LGE patterns based on the American Heart Association (AHA) 17-segment model[21]. LGE was defined using a signal intensity threshold of 5 standard deviations (SDs) above that of a remote myocardial region, which served as a reference within the same section[22]

Mitral regurgitation volume was determined by subtracting the forward aortic flow volume from the LV stroke volume. The mitral regurgitation fraction was calculated by dividing the mitral regurgitation volume by the LV stroke volume. Mitral regurgitation severity was categorized as follows: 0 (none to trace) for 0% to 5%, 1+ (mild) for <15-20%, 2+ (moderate) for 20% to 40%, 3+ (severe) > 40 %, and 4+ (very severe) for values greater than 50%[23,24].

Reproducibility

To evaluate intra-observer variability, an experienced observer re-analyzed a random subset of 20 patients, including cases of NA-STEMI with and without PPM infarction, after a minimum interval of six weeks. To assess inter-observer variability, a second blinded observer with two years of experience in cardiovascular imaging independently performed the same post-processing analysis on the same subset of 20 patients without access to the initial results.

Statistical analysis

Continuous variables are presented as mean ± standard deviation. Comparisons of continuous data were performed using the independent samples t-test or Mann-Whitney U test; Kolmogorov-Smirnov tests were used to check continuous variables for normal distribution. Categorical variables were compared by using the chi-square test or Fisher's exact test, as appropriate. Correlation was assessed using the Pearson r and Spearman rho coefficient as appropriate. Intraobserver and inter- observer variability were assessed by intraclass correlation coefficients.

Association between papillary muscle infarction, clinical and CMR parameters, and myocardial infarction were analyzed using multivariable linear regression. Atrial and ventricular strain determinants that demonstrated statistical significance ($p < 0.05$) during univariable analysis were subjected to further examination through multivariable linear regression, adjusting for all factors that were statistically significant in the univariable analysis.

A p-value <0.05 was considered statistically significant. All statistical analysis was performed using Jeffreys's Amazing Statistics Program (JASP) software.

Results

Baseline characteristics

A total of 88 patients with NA-STEMI, comprising 68 males (77.27%) and 20 females (22.73%) with a mean age of 65 ± 10.05 years, were included. The patients enrolled were divided into two distinct groups based on PPM involvement by LGE. One group comprised 30 patients with papillary muscle LGE confirmed in two orthogonal slices (25 males, 83.33%; mean age 67.12 ± 9.49 years), and the other group comprised 58 patients without PPM LGE (43 males, 74.14%; mean age 60.90 ± 10 years). Patients with papillary muscle infarction were older and had more cardiovascular risk factors, including smoking ($p = 0.011$), obesity ($p = 0.021$), and a family history of coronary artery diseases ($p = 0.009$), in comparison to NA-STEMI patients without PPM involvement by LGE.

Table 1 displays the comparison among the groups enrolled

CMR features in NA-STEMI patients.

CMR characteristics of the enrolled patients are summarized in **Table 2**. NA-STEMI patients with PPM infarction showed a lower LV ejection fraction (34.18 ± 9.20 vs. 39.15 ± 12.70, p = 0.040) and higher end-diastolic and end-systolic indexed left ventricle volumes (123.55 ± 24.69 vs. 111.90 ± 39.79, p = 0.020; 81.46 ± 26.17 vs. 71.61 ± 37.27, p = 0.044, respectively). Conversely, no significant differences were found in the right ventricle volumes and functions. Among the PPMs affected by LGE, the postero-medial was the most commonly involved (19 patients, 63%), while the antero-lateral was involved in 4 patients (13%). Both PPMs were affected in 7 patients (23%) No differences were observed in the presence and severity of mitral valve regurgitation between patients with and without PPM infarction (p = 0.446 and p = 0.723, respectively). Regarding the degree of mitral regurgitation, in the PPM infarction group, 16 (53%) patients had mild mitral regurgitation, and 2 (7%) had moderate regurgitation. Conversely, among NA-STEMI patients without PPM involvement, 30 (52%) had mild mitral regurgitation, and 11 (18%) had moderate regurgitation. None of the patients in either group demonstrated severe mitral regurgitation. Patients with PPM infarction demonstrated lower reservoir and booster strain parameters (11.33 ± 5.33 vs. 21.21 ± 10.60, p = 0.001 and 8.71 ± 5.98 vs. 11.74 ± 6.27, p = 0.004, respectively). Regarding ventricular strain parameters, GLS showed more impaired values compared to NA-STEMI patients without PPM infarction (-8.7 ± 2.58 vs. -10.07 ± 4.2, p = 0.001). Moreover, a more extensive myocardial LGE was observed in NA-STEMI patients with PPM infarction, with a mean myocardial segment involvement of 7.01 ± 2.43 segments compared to 5.31 ± 2.22 segments in patients without LGE in PPM (p = 0.002).

Correlation between atrial and ventricular strain and other CMR parameters

In **Figure 3** the correlation matrix shows the demographic and CMR characteristics of NA-STEMI patients and their association with LA and LV strains.

All LV strains were significantly correlated with LV end-diastolic volume index (GCS: R=0.43 p=0.001; GRS: R=-0.42 p=0.001; GLS: R=0.36 p=0.001), LV end-systolic volume index (GCS: R=0.55 p=0.001 ; GRS: R=-0.55 p=0.001; GLS: R=0.47 p=0.001), LV stroke volume index (GCS: R=- 0.31 p=0.001; GRS: R=0.29 p=0.001; GLS: R=-0.25 p=0.001), and LV EF (GCS: R=-0.74 p=0.001; GRS: R=0.72 p=0.001; GLS: R=-0.66 p=0.001).

Regarding LA strain parameters, reservoir significantly correlated with LV EF (R=0.51, p=0.001), LV end-diastolic volume index (R=- 0.25, p=0.026), LV end-systolic volume index (R=-0.34, p=0.002), and LV stroke volume index (R=0.25, p=0.022). Conduit strain significantly correlated with LV EF (R=0.51, p=0.001), LV end-systolic volume index (R=-0.34, p=0.002), and LV stroke volume index (R=0.41, p=0.001). Finally, booster strain significantly correlated with LV EF (R=0.51, p=0.001), LV end-diastolic volume index (R=- 0.25, p=0.024), LV end-systolic volume index (R=-0.34, p=0.008).

All LV strains were significantly correlated with each other (GCS and GRS: R=-0.92 p=0.001; GCS and GLS: R=0.72 p=0.001; GRS and GLS: R=-0.68 p=0.001) and with reservoir and conduit strain parameters(GCS and reservoir: R=-0.43, p=0.001; GRS and reservoir: R=0.45, p=0.001; GLS and reservoir: R=-0.66, p=0.001; GCS and conduit: R=-0.50, p=0.001; GRS and conduit: R=0.51, p=0.001; GLS and conduit: R=-0.60, p=0.001)

Papillary muscle infarction correlated with all LV and LA strain parameters (GCS: R=-0.17 , p=0.049; GRS: R=-0.26 , p=0.013; GLS: R=-0.17 , p=0.001; Reservoir: R=-0.47 , p=0.001; Conduit: R=-0.21 , p=0.049; Booster: R=-0.27 , p=0.013)

Determinant of papillary muscle infarction in NA-STEMI patients

Univariable and multivariable determinants of PPM infarction are presented in **Table 3** and **Table 4**. Univariable analysis revealed that age, smoke, obesity, familiarity of coronary artery disease,

reservoir, booster, GLS, and GRS as well as the number of myocardial segments involved by LGE were independently associated with PPM infarction (β coefficient = -2.638, p = 0.008; β coefficient = 1.996, p = 0.046; β coefficient = 2.539, p = 0.011; β coefficient = -3.865, p = 0.001; β coefficient = -2.391, p = 0.017; β coefficient = 3.190, p = 0.001; β coefficient = -2.335, p = 0.020; β coefficient = 2.923, p = 0.003, respectively). Further multivariable analysis revealed that reservoir, booster, GLS, and GRS were the only independent determinant of PPM infarction (β coefficient = -3.401, p = 0.001; β coefficient = -2.048, p = 0.041; β coefficient = 3.10, p = 0.001; β coefficient = -2.212, p = 0.027)

Reproducibility

The intra-observer and inter-observer agreement for atrial and ventricular strain parameters was good. Intraclass correlation coefficients ranged from 0.86 to 0.95 for intra-observer agreement and from 0.81 to 0.90 for inter-observer agreement

Discussion

The main findings of this study were as follows: (1) Patients with PPM infarction were older and had higher left ventricular end-diastolic and end-systolic volumes; (2) In patients with PPM infarction, both atrial and ventricular strain parameters were impaired; (3) GLS, GRS, reservoir, and booster strain parameters were independently associated with PPM infarction.

PPM infarction is a well-documented complication after myocardial infarction because the primary artery supplying the PPMs is a terminal artery[25]. Ischemia that disrupts the blood supply to the papillary muscles can lead to infarction and subsequent dysfunction of these muscles[20].

Echocardiography is the preferred method for evaluating PPM morphology and function; however, visually confirming papillary muscle infarction with this technique is very challenging[26].

PPM infarction can be detected noninvasively in clinical settings using CMR in vivo. CMR sequences with gadolinium administration can identify myocardial fibrosis as well as PPM fibrosis, which is indicative of infarction[27–30].

Patients with PPM infarction demonstrated a more impaired LV ejection fraction and higher LV volumes. These findings are in line with the literature[3,20]. Eitel et al. explored the role of PPM in a multicenter study of 738 reperfused STEMI patients, reporting impaired LV function in patients with PPM infarction[20]. Indeed, a strict interrelationship between LV volume, stroke volume, and PPM exists, as reported in the transesophageal echocardiographic study by Madu et al[31].

Furthermore, our findings of no significant differences in the presence and severity of MR in patients with PPM infarction are consistent with the understanding that PPM infarction is not directly associated with the development or severity of mitral regurgitation[3,20,32]. Instead, PM infarction is linked to LV remodeling, increased mitral annular dilation, systolic retraction of the mitral leaflets, and reduced coaptation. The development of MR is likely mediated by infarct location, particularly in the lateral wall, and LV remodeling, leading to secondary dysfunction of the mitral valve apparatus, rather than by the PM infarction itself[32].

Additionally, in patients with PPM infarction, GLS demonstrated lower values compared to STEMI patients without PPM involvement and is independently linked to the presence of PPM infarction, which could be related to the role of the PPM in LV contraction. PPMs connect the LV wall to the mitral valve via the chordae tendineae. This subvalvular apparatus functions along the longitudinal axis of the left ventricle, parallel to the LV wall, making it an integral part of the longitudinal function of the left ventricle. Dysfunction of the PPMs can lead to changes in LV shape and reduced performance[33,34]. The myocardium consists of various layers, each with distinct myofiber orientations. GLS measures the shortening of subendocardial fibers along the longitudinal axis, from the base to the apex[35,36]. Another independent determinant of PPM is GRS, which reflects the thickening and thinning of the myocardium, encompassing both the subepicardial and subendocardial layers, in a radial direction towards the center of the LV. This is likely because LV

performance dysfunction due to PPM infarction is not limited to the subendocardial layer but more extensively affects the myocardial fibers.

Another notable finding was the observation of impaired atrial function in STEMI patients with PPM infarction. The papillary muscles and their chordae regulate the closure of the atrioventricular valve during systole, influencing atrial performance[11,13,37,38]. The left atrium is an active cardiac chamber that centrally regulates cardiac output by modulating LV filling through three distinct phases: reservoir, conduit, and booster[13]. STEMI patients with PPM involvement exhibited more impaired reservoir and booster strain. Reservoir strain primarily represents atrial relaxation and compliance, influenced by the descent of the mitral anulus during systole[39], which is affected by PPM dysfunction. Whereas booster strain parameters reflect intrinsic atrial contractility, which is modulated by the degree of venous return, as well as LV diastolic compliance and pressure. Given the impairment of LV performance, the impaired reservoir and booster strain are expected because the ventricle and the atrium are anatomically linked.

Recent advances in CMR imaging, particularly novel techniques such as T1 and T2 mapping, offer promising avenues for enhancing the assessment of PPM infarction. These recently introduced techniques may provide valuable insights into myocardial tissue changes in patients with PPM infarction and their relationship with atrial and ventricular impairment in this subgroup of ischemic patients. Future studies should explore how T1 and T2 mapping can be used to improve the evaluation of PPM infarction and its impact on myocardial strain, with the goal of enhancing patient outcomes through earlier and more accurate detection of myocardial injury.

Clinical implications

Our study highlights the significant pathophysiological role of PPM infarction in NA-STEMI patients, an often overlooked finding in CMR reports. The presence of LGE in the PPM was independently associated with greater impairment of both atrial and ventricular strain compared to STEMI patients without PPM involvement. These findings support the important contribution of

PPM to atrial and ventricular performance and suggest their importance in PPM dysfunction due to infarction. The identification of PPM infarction and its association with impaired atrial and ventricular strain could potentially lead to earlier therapeutic interventions and improved risk stratification for NA-STEMI patients. Future studies should investigate whether targeted interventions aimed at preserving PPM function can improve outcomes in this patient population.

Limitations

This study has several limitations that need to be acknowledged. First, the sample size is relatively small, which may limit the generalizability of the findings and reduce the statistical power of our analyses. Furthermore, atrial and ventricular strain analyses were performed for each patient using a validated post-processing software and a standardized acquisition protocol. While this approach minimizes measurement variability, it may also limit the generalizability of the findings. Although our results are promising, further research with a larger patient population and a multicenter design is needed to validate our findings.

Secondly, the study employed a cross-sectional design, which precludes the assessment of the predictive value of PPM infarction for adverse cardiovascular events in patients with NA-STEMI. Additionally, changes in atrial and ventricular strain parameters over time were not examined. Moreover, the absence of quantitative edema data through T2 mapping assessment, which could provide valuable information on ventricular strain, represents another potential limitation of the study. Furthermore, the limited sensitivity of conventional LGE CMR for detecting PPM infarction is a concern, and gray-blood LGE CMR was not performed in this study. Future longitudinal studies are required to evaluate the prospective association of this CMR parameter with patient outcomes and to investigate quantitative changes in atrial and ventricular function over time.

Conclusion

PPM infarction in NA-STEMI patients detected by LGE-CMR sequences is independently linked to atrial and ventricular strain parameters, confirming the impact of PPM on left atrial and ventricular performance.

Conflicts of Interest: Nothing to Disclose.

Data availability: All data are available from the corresponding author on request.

References

1. Hansen DE, Cahill PD, DeCampli WM, et al. Valvular-ventricular interaction: importance of the mitral apparatus in canine left ventricular systolic performance. *Circulation*. 1986;73(6):1310-1320.
2. Athanasiou T, Chow A, Rao C, et al. Preservation of the mitral valve apparatus: evidence synthesis and critical reappraisal of surgical techniques. *European journal of cardio-thoracic surgery*. 2008;33(3):391-401.
3. Tanimoto T, Imanishi T, Kitabata H, et al. Prevalence and Clinical Significance of Papillary Muscle Infarction Detected by Late Gadolinium-Enhanced Magnetic Resonance Imaging in Patients With ST-Segment Elevation Myocardial Infarction. *Circulation*. 2010;122(22):2281-2287. doi:10.1161/CIRCULATIONAHA.109.935338
4. Rajiah P, Fulton NL, Bolen M. Magnetic resonance imaging of the papillary muscles of the left ventricle: normal anatomy, variants, and abnormalities. *Insights Imaging*. 2019;10(1):83. doi:10.1186/s13244-019-0761-3
5. Wendell D, Jenista E, Kim HW, et al. Assessment of Papillary Muscle Infarction with Dark-Blood Delayed Enhancement Cardiac MRI in Canines and Humans. *Radiology*. 2022;305(2):329-338. doi:10.1148/radiol.220251
6. Hou J, Sun Y, Wang H, Zhang L, Yang B. Papillary Muscle Infarction by Cardiac MRI in Patients With Mitral Regurgitation. *Clin Cardiol*. 2024;47(7):e24312. doi:https://doi.org/10.1002/clc.24312
7. Onnis C, Muscogiuri G, Paolo Bassareo P, et al. Non-invasive coronary imaging in patients with COVID-19: A narrative review. *Eur J Radiol*. 2022;149:110188. doi:10.1016/j.ejrad.2022.110188
8. Muscogiuri G, Guglielmo M, Serra A, et al. Multimodality Imaging in Ischemic Chronic Cardiomyopathy. *J Imaging*. 2022;8(2). doi:10.3390/jimaging8020035
9. Muscogiuri G, Volpato V, Cau R, et al. Application of AI in cardiovascular multimodality imaging. *Heliyon*. Published online 2022:e10872. doi:https://doi.org/10.1016/j.heliyon.2022.e10872
10. Fahmy AS, Neisius U, Tsao CW, et al. Gray blood late gadolinium enhancement cardiovascular magnetic resonance for improved detection of myocardial scar. *Journal of Cardiovascular Magnetic Resonance*. 2018;20(1):22. doi:10.1186/s12968-018-0442-2

11. Meloni A, Saba L, Positano V, et al. Left atrial strain in patients with β-thalassemia major: a cross-sectional CMR study. *Eur Radiol*. Published online March 2024. doi:10.1007/s00330-024-10667-x
12. Cau R, Pisu F, Muscogiuri G, et al. Atrial and ventricular strain using cardiovascular magnetic resonance in the prediction of outcomes of pericarditis patients: a pilot study. *Eur Radiol*. Published online 2024. doi:10.1007/s00330-024-10677-9
13. Cau R, Bassareo P, Suri JS, Pontone G, Saba L. The emerging role of atrial strain assessed by cardiac MRI in different cardiovascular settings: an up-to-date review. *Eur Radiol*. 2022;32(7):4384-4394. doi:10.1007/s00330-022-08598-6
14. Cau R, Pisu F, Porcu M, et al. Machine learning approach in diagnosing Takotsubo cardiomyopathy: The role of the combined evaluation of atrial and ventricular strain, and parametric mapping. *Int J Cardiol*. Published online November 2022. doi:10.1016/j.ijcard.2022.11.021
15. Thygesen K, Alpert JS, Jaffe AS, et al. Fourth universal definition of myocardial infarction (2018). *Eur Heart J*. 2019;40(3):237-269. doi:10.1093/eurheartj/ehy462
16. Huang X, Redfors B, Chen S, et al. Predictors of mortality in patients with non-anterior ST-segment elevation myocardial infarction: Analysis from the HORIZONS-AMI trial. *Catheterization and Cardiovascular Interventions*. 2019;94(2):172-180. doi:https://doi.org/10.1002/ccd.28096
17. Unger T, Borghi C, Charchar F, et al. 2020 International Society of Hypertension Global Hypertension Practice Guidelines. *Hypertension*. 2020;75(6):1334-1357. doi:10.1161/HYPERTENSIONAHA.120.15026
18. Organization WH. Definition and diagnosis of diabetes mellitus and intermediate hyperglycaemia: report of a WHO/IDF consultation. Published online 2006.
19. Flegal KM, Carroll MD, Kuczmarski RJ, Johnson CL. Overweight and obesity in the United States: prevalence and trends, 1960–1994. *Int J Obes*. 1998;22(1):39-47.
20. Eitel I, Gehmlich D, Amer O, et al. Prognostic Relevance of Papillary Muscle Infarction in Reperfused Infarction as Visualized by Cardiovascular Magnetic Resonance. *Circ Cardiovasc Imaging*. 2013;6(6):890-898. doi:10.1161/CIRCIMAGING.113.000411
21. Imaging: AHAWG on MS and R for C, Cerqueira MD, Weissman NJ, et al. Standardized Myocardial Segmentation and Nomenclature for Tomographic Imaging of the Heart. *Circulation*. 2002;105(4):539-542. doi:10.1161/hc0402.102975
22. Moon JC, Messroghli DR, Kellman P, et al. Myocardial T1 mapping and extracellular volume quantification: a Society for Cardiovascular Magnetic Resonance (SCMR) and CMR Working Group of the European Society of Cardiology consensus statement. *Journal of Cardiovascular Magnetic Resonance*. 2013;15(1):92. doi:10.1186/1532-429X-15-92
23. Gelfand E V, Hughes S, Hauser TH, et al. Severity of Mitral and Aortic Regurgitation as Assessed by Cardiovascular Magnetic Resonance: Optimizing Correlation with Doppler Echocardiography. *Journal of Cardiovascular Magnetic Resonance*. 2006;8(3):503-507. doi:10.1080/10976640600604856
24. Myerson SG. CMR in Evaluating Valvular Heart Disease: Diagnosis, Severity, and Outcomes. *JACC Cardiovasc Imaging*. 2021;14(10):2020-2032. doi:https://doi.org/10.1016/j.jcmg.2020.09.029
25. Madu EC, D'Cruz IA. The vital role of papillary muscles in mitral and ventricular function: echocardiographic insights. *Clin Cardiol*. 1997;20(2):93-98. doi:https://doi.org/10.1002/clc.4960200203

26. Agricola E, Oppizzi M, Pisani M, Meris A, Maisano F, Margonato A. Ischemic mitral regurgitation: mechanisms and echocardiographic classification. *European Journal of Echocardiography*. 2008;9(2):207-221. doi:10.1016/j.euje.2007.03.034
27. Cau R, Solinas C, De Silva P, et al. Role of cardiac MRI in the diagnosis of immune checkpoint inhibitor-associated myocarditis. *Int J Cancer*. Published online June 2022. doi:10.1002/ijc.34169
28. Cau R, Muscogiuri G, Pisu F, et al. Effect of late gadolinium enhancement on left atrial impairment in myocarditis patients. *Eur Radiol*. 2023;(0123456789). doi:10.1007/s00330-023-10176-3
29. Cau R, Loewe C, Cherchi V, et al. Atrial Impairment as a Marker in Discriminating Between Takotsubo and Acute Myocarditis Using Cardiac Magnetic Resonance. *J Thorac Imaging*. 2022;37(6):W78-W84. doi:10.1097/RTI.0000000000000650
30. Weng Z, Yao J, Chan RH, et al. Prognostic Value of LGE-CMR in HCM: A Meta-Analysis. *JACC Cardiovasc Imaging*. 2016;9(12):1392-1402. doi:10.1016/j.jcmg.2016.02.031
31. Madu EC, Baugh DS, Johns C, D'Cruz IA. Papillary Muscle Contribution to Ventricular Ejection in Normal and Hypertrophic Ventricles: A Transesophageal Echocardiographic Study. *Echocardiography*. 2001;18(8):633-638. doi:https://doi.org/10.1046/j.1540-8175.2001.00633.x
32. Bax JJ, Delgado V. Papillary Muscle Infarction, Mitral Regurgitation, and Long-Term Prognosis. *Circ Cardiovasc Imaging*. 2013;6(6):855-857. doi:10.1161/CIRCIMAGING.113.000986
33. Hansen DE, Cahill PD, DeCampli WM, et al. Valvular-ventricular interaction: importance of the mitral apparatus in canine left ventricular systolic performance. *Circulation*. 1986;73(6):1310-1320. doi:10.1161/01.CIR.73.6.1310
34. Jones CJ, Raposo L, Gibson DG. Functional importance of the long axis dynamics of the human left ventricle. *Br Heart J*. 1990;63(4):215. doi:10.1136/hrt.63.4.215
35. Scatteia A, Baritussio A, Bucciarelli-Ducci C. Strain imaging using cardiac magnetic resonance. *Heart Fail Rev*. 2017;22(4):465-476. doi:10.1007/s10741-017-9621-8
36. Cau R, Bassareo P, Cademartiri F, et al. Epicardial fat volume assessed with cardiac magnetic resonance imaging in patients with Takotsubo cardiomyopathy. *Eur J Radiol*. 2023;160:110706. doi:10.1016/j.ejrad.2023.110706
37. Meloni A, Saba L, Positano V, et al. Left and right atrioventricular coupling index in patients with beta-thalassemia major. *Int J Cardiovasc Imaging*. Published online 2024. doi:10.1007/s10554-024-03146-3
38. Cau R, Bassareo P, Caredda G, Suri JS, Esposito A, Saba L. Atrial Strain by Feature-Tracking Cardiac Magnetic Resonance Imaging in Takotsubo Cardiomyopathy. Features, Feasibility, and Reproducibility. *Can Assoc Radiol J*. Published online October 2021:8465371211042497. doi:10.1177/08465371211042497
39. Nagueh SF, Khan SU. Left Atrial Strain for Assessment of Left Ventricular Diastolic Function: Focus on Populations With Normal LVEF. *JACC Cardiovasc Imaging*. 2023;16(5):691-707. doi:10.1016/j.jcmg.2022.10.011

Figure legends.

Figure 1: Flowchart of the patients enrolled.

Figure 2: Representative atrial and ventricular strain parameters impairment in NA-STEMI with and without papillary muscle infarction detected by late gadolinium enhancement images. Short-axis and 4-chamber LGE images in patients with NA-STEMI involving the left circumflex artery with papillary muscle infarction are shown (arrows in Panels A and B). Atrial and ventricular strain parameters and their corresponding curves are reported in Panels C, D, E, and F. Short-axis and 2-chamber LGE images in patients with NA-STEMI involving the right coronary artery without papillary muscle infarction are shown in Panels G and H. Atrial and ventricular strain parameters and their corresponding curves are reported in Panels I, J, K, and L

Figure 3: The correlation heat map of left ventricle and left atrium strain parameters with CMR characteristics.

Tables

Variables	Papillary muscle infarction (30 patients)	No papillary muscle infarction (58 patients)	p- values
Sex (male)	25 (83%)	43 (74%)	0.335
Age (years)	67.12 ± 9.49	60.90 ± 10	**0.006**
Hypertension, n (%)	20 (66%)	37 (63%)	0.715
Dyslipidemia, n (%)	12 (40%)	22 (38%)	0.855
Smoke, n (%)	20 (66%)	22 (38%)	**0.011**
Obesity, n (%)	13 (22%)	1 (3%)	**0.021**
Diabetes, n (%)	8 (27%)	14 (24%)	0.801
Familiarity for CAD, n (%)	10 (33%)	6 (10%)	**0.009**

Table 1: Baseline characteristics of patients with and without papillary muscle infarction.

Abbreviations: CAD coronary artery disease

Variables	Papillary muscle infarction	No papillary muscle infarction	p- values
LVEF, %	34.18 ± 9.20	39.15 ± 12.70	**0.040**
LVEDV/BSA, mL/m2	123.55 ± 24.69	111.90 ± 39.79	**0.020**
LVESV/BSA, mL/m2	81.46 ± 26.17	71.61 ± 37.27	**0.044**
LVSV/BSA, mL/m2	41.99 ± 11.11	40.23 ± 12.47	0.617
RVEF, %	52.04 ± 11.50	51.55 ± 13.83	0.984
RVEDV/BSA, mL/m2	71.40 ± 17.31	65.79 ± 21.59	0.165
RVESV/BSA, mL/m2	35.31 ± 15.78	33.02 ± 16.21	0.367
RVSV/BSA, mL/m2	35.43 ± 9.88	33.21 ± 11.74	0.387
Mitral regurgitation, n (%)	18 (60%)	30 (52%)	0.446
Reservoir, %	11.33 ± 5.33	21.21 ± 10.60	**0.001**
Conduit, %	6.22 ± 2.99	8.97 ± 7	0.074
Booster, %	8.71 ± 5.98	11.74 ± 6.27	**0.004**
GLS, %	-8.7 ± 2.58	-10.07 ± 4.2	**0.001**
GCS, %	6.79 ± 2.31	-9.73 ± 4.1	0.175
GRS, %	11.98 ± 4.01	16.23 ± 8.74	0.052

LGE extent, number of segments	7.01 ± 2.43	5.31 ± 2.22	**0.002**

Table 2: CMR findings of NA-STEMI patients with and without papillary muscle infarction

Abbreviations: BSA, body surface area; EDV, end-diastolic volume; ESV, end-systolic volume; LGE, late gadolinium enhancement; LV, left ventricle; SV, stroke volume; RV, right ventricle.

Variables	Univariable	
	β coefficent	*p values*
Sex	-0.968	0.333
Age	2.638	**0.008**
Hypertension	0.919	0.417
Dyslipidemia	0.189	0.850
Smoke	2.509	**0.012**
Obesity	-1.996	**0.046**
Diabetes	0.260	0.795
Familiarity for CAD	2.530	**0.011**
LVEF	1.840	0.066
LVEDV/BSA	1.384	0.166
LVESV/BSA	1.213	0.218
LVSV/BSA	0.636	0.525

RVEF	0.164	0.869
RVEDV/BSA	1.192	0.233
RVESV/BSA	0.638	0.533
RVSV/BSA	0.828	0.408
Mitral regurgitation	0.738	0.461
Reservoir	-3.865	**0.001**
Conduit	-1.901	0.057
Booster	-2.391	**0.017**
GLS	3.190	**0.001**
GCS	1.586	0.113
GRS	-2.335	**0.020**
LGE extent	2.923	**0.003**

Table 3: Univariable analysis of determinants of papillary muscle infarction in NA-STEMI patients.

Abbreviations: BSA, body surface area; CAD coronary artery disease; EDV, end-diastolic volume; ESV, end-systolic volume; LGE, late gadolinium enhancement; LV, left ventricle; STIR, short tau inversion recovery; SV, stroke volume; RV, right ventricle.

Variables	Multivariable

	β coefficent	*p values*
Reservoir, %	-3.401	**0.001**
Booster, %	-2.048	**0.041**
GLS, %	3.10	**0.002**
GRS, %	-2.212	**0.027**

Table 4: Multivariables analysis of determinants of papillary muscle infarction in NA-STEMI patients

All myocardial strain parameters were adjusted for factors that were statistically significant in the univariable analysis.

Figures

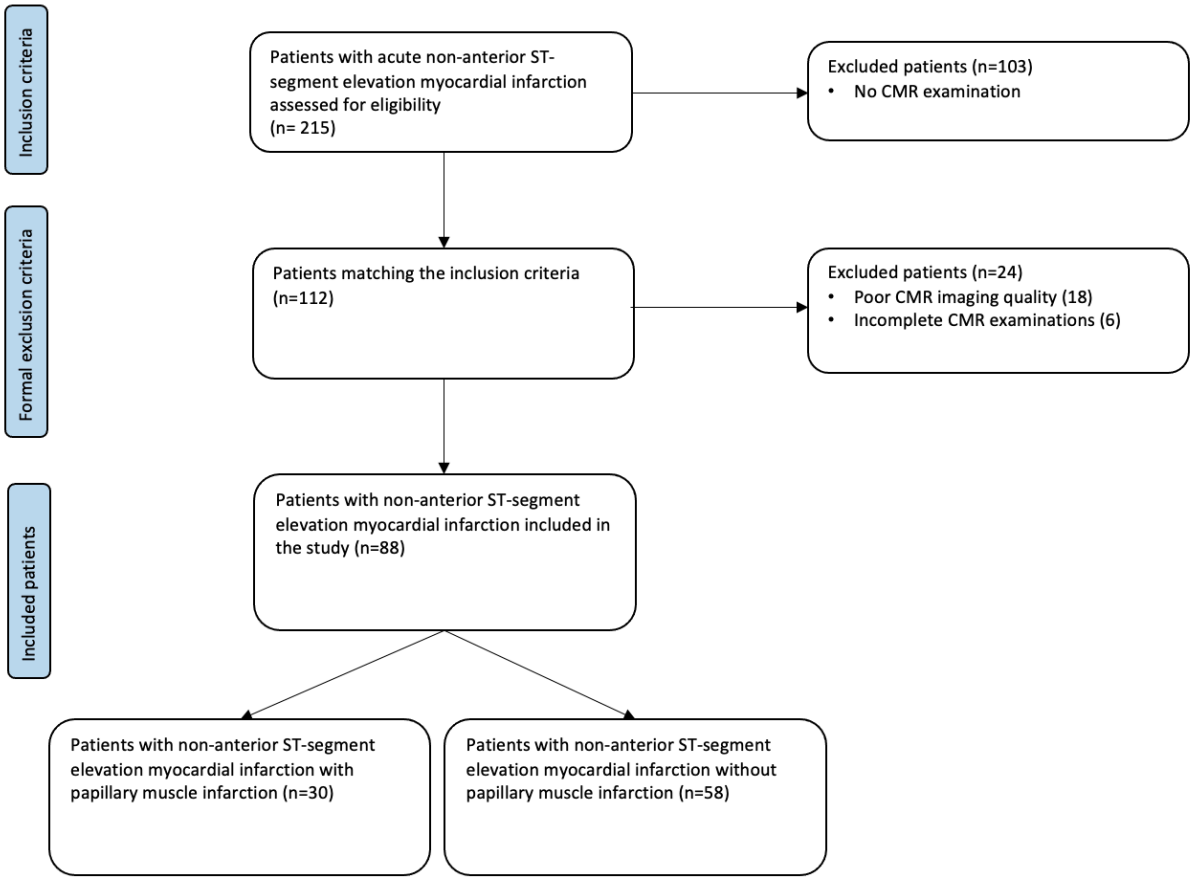

Figure 1: Flowchart of the patients enrolled.

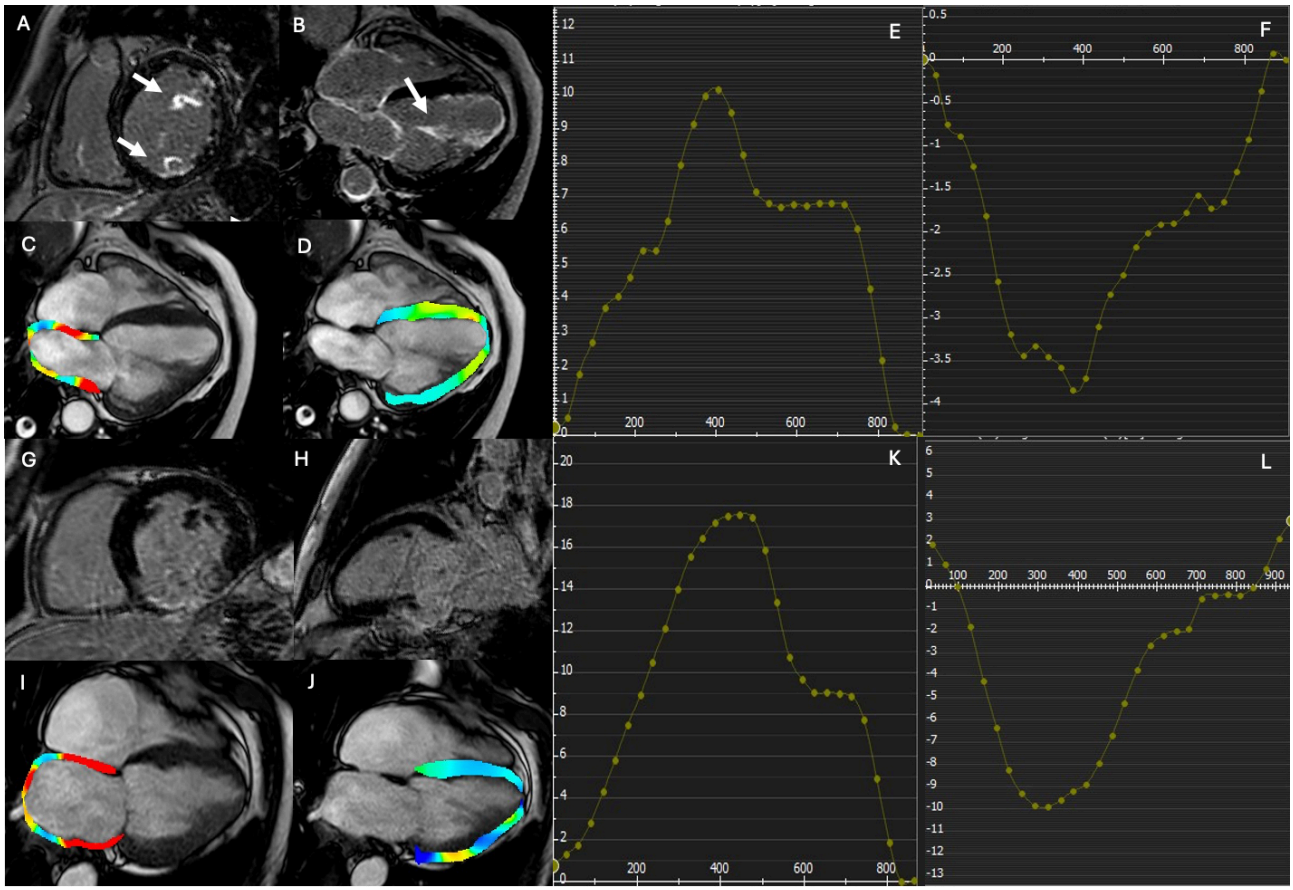

Figure 2: Representative atrial and ventricular strain parameters impairment in NA-STEMI with and without papillary muscle infarction detected by late gadolinium enhancement images. Short-axis and 4-chamber LGE images in patients with NA-STEMI involving the left circumflex artery with papillary muscle infarction are shown (arrows in Panels A and B). Atrial and ventricular strain parameters and their corresponding curves are reported in Panels C, D, E, and F. Short-axis and 2-chamber LGE images in patients with NA-STEMI involving the right coronary artery without papillary muscle infarction are shown in Panels G and H. Atrial and ventricular strain parameters and their corresponding curves are reported in Panels I, J, K, and L

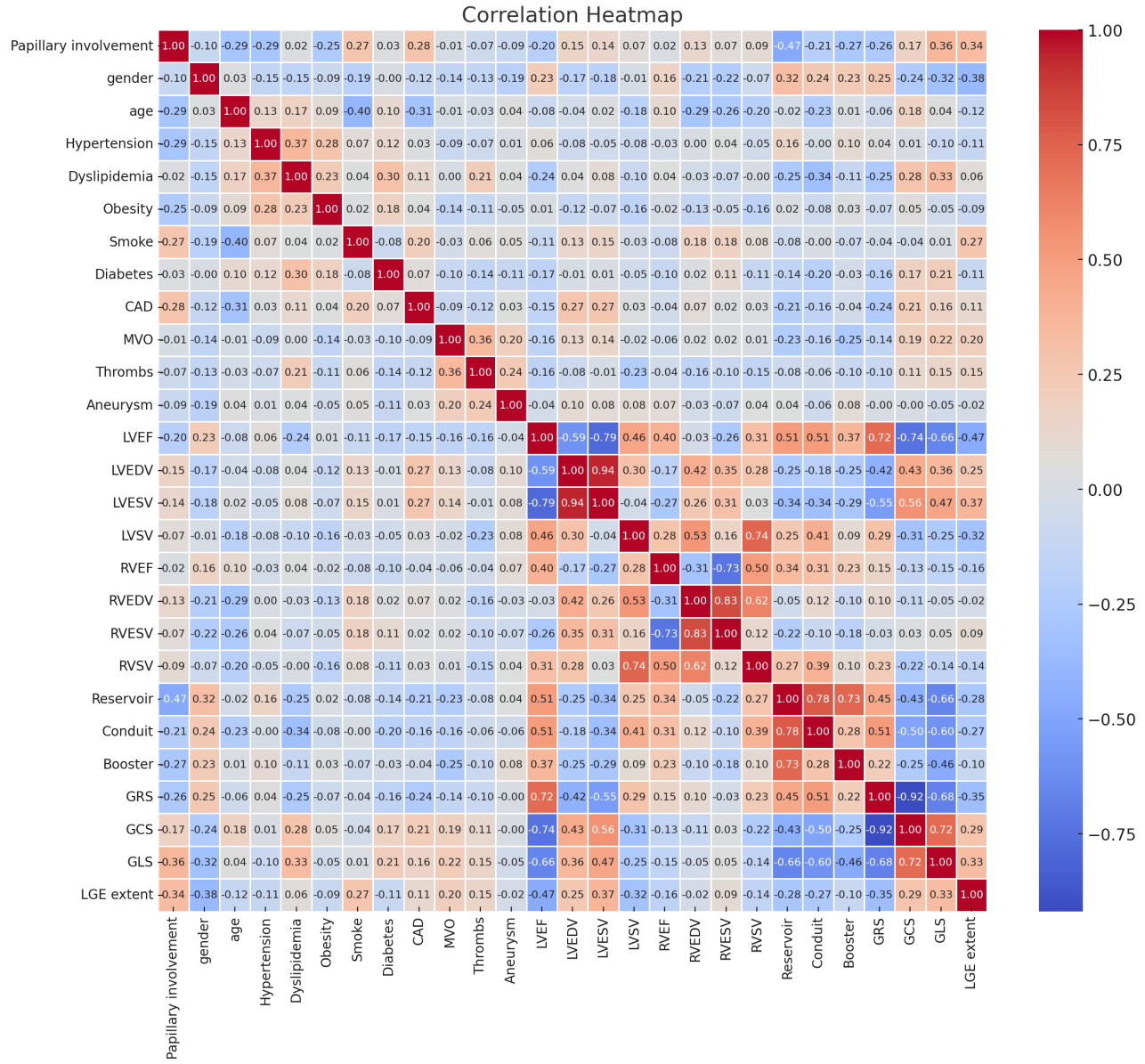

Figure 3: The correlation heat map of left ventricle and left atrium strain parameters with CMR characteristics.